Modification of Acrylonitrile–Butadiene–Styrene Terpolymer by Graft Copolymerization with Maleic Anhydride in the Melt. II. Properties and Phase Behavior

Rongrong Qi, Junling Qian, Zhefeng Chen, Xing Jin, Chixing Zhou

School of Chemistry and Chemical Engineering, Shanghai Jiao Tong University, Shanghai 200240, China

Received 4 February 2003; accepted 4 August 2003

ABSTRACT: The graft copolymerization of maleic anhydride (MAH) onto acrylonitrile–butadiene–styrene terpolymer (ABS) using dicumyl peroxide and benzoyl peroxide as the binary initiator and styrene as the comonomer in the molten state was described. The properties and phase morphologies of the modified products (ABS-*g*-MAH) were studied. The results indicate that the melt flow index (MFI) of ABS-*g*-MAH increases with the increase of MAH content, the initiator concentration, and the screw speed, whereas the MFI decreases with the increase of temperature. The impact strength and the percentage elongation of ABS-*g*-MAH both decreased and the tensile strength of ABS-*g*-MAH increased slightly as the grafting degree increased. The phase inversion behavior of the modified product was observed by transmission electron microscopy. © 2004 Wiley Periodicals, Inc. J Appl Polym Sci 91: 2834–2839, 2004

Key words: ABS-*g*-MAH; melt flow index (MFI); mechanical properties; phase behavior; graft copolymers

INTRODUCTION

The development of useful polymer blends has been the subject of intensive investigation in recent years because of their growing commercial acceptance. However, immiscible blends often exhibit poor mechanical properties and have unstable phase morphology during melt processing. Adding a proper compatibilizer is an effective way to solve the problem associated with incompatible polymer mixtures. Some functionalized polymers have been widely used as reactive compatibilizers of polymer blends in various applications.[1] In general, functionalized polymers can be obtained by graft copolymerization of functional monomers with some commercially available polymers such as polybutadiene (PB), styrene–butadiene block copolymers (SBS), and acrylonitrile–butadiene–styrene (ABS) terpolymer.[2–11] For example, Abdel-Razik et al.[12,13] investigated the photoinduced graft copolymerization of acrylamide onto ABS in chloroform in the presence of benzophenone or 4-acetyldiphenyl. Oxazoline-functionalized ABS was also reported by La Mantia et al.[14] and Mülhaupt et al.[15]

It is well known that a grafting polymerization will become efficient only when the number of grafted units is adequate and the side reactions (e.g., crosslinking, degradation, etc.) are almost absent[16] because usually both the grafting and side reactions lead to significant changes of the grafted copolymers' properties such as melt flow index, soluble fraction of the graft copolymer,[17] and phase behavior. As a compatibilizer of polymer blends, not only grafting degree but also the graft copolymers' properties and phase behavior would have an effect on the properties of the immiscible polymer blends. Therefore, it is important to investigate the grafted copolymers' properties and phase behavior, although only a few investigations have been reported to date. On the other hand, with styrene as the comonomor, an attempt to obtain a higher grafting degree of maleic anhydride onto ABS terpolymer by using binary initiator [dicumyl peroxide + benzoyl peroxide (DCP + BPO)] in the melt was previously reported in detail.[18] The present work is mainly focused on the investigation of their properties and phase behavior.

EXPERIMENTAL

Materials

ABS (M_n = 49,000, M_w = 134,000, M_w/M_n = 2.72, containing 2.7 wt % additives, 22.4 wt % acrylonitrile, 13.5 wt % butadiene, and 61.4 wt % styrene, determined by elemental analysis and solvent separation method) was purchased from Taiwan Qimei Co. (Taipei, China). BPO (Shanghai Lingfeng Chemical Solvent Factory, China) was purified by dissolving in chloroform at room temperature and precipitating in

Correspondence to: R. Qi (rrqi@sjtu.edu.cn).

Contract grant sponsor: Natural Science Foundation of China; contract grant number: 50390095.

Journal of Applied Polymer Science, Vol. 91, 2834–2839 (2004)

cool methanol. DCP and maleic anhydride (MAH; Shanghai Chemical Solvent Factory) were used without further purification. Styrene was purified by distillation under reduced pressure at 30°C.

Preparation and purification of grafted copolymers

The grafting reaction was carried out in the molten state using a Haake twin-screw extruder (Haake, Bersdorff, Germany) under various processing conditions. In a typical process, ABS, MAH, initiators, solvent, and comonomors were premixed at room temperature, after which 60 g of premixed materials was added to the extruder. The grafting product was dissolved in 1,2-dichloroethane and the unreacted MAH in the solution was extracted with ethanol. The purified polymer was collected and dried to constant weight in a vacuum oven at 80°C.

FTIR characterization of grafted copolymers

Samples were cast into films (0.010–0.015mm thick) using chloroform as solvent. IR spectroscopic information on ABS and grafted ABS were obtained using a Perkin–Elmer Paragon 1000 FTIR spectrophotometer (Perkin Elmer Cetus Instruments, Norwalk, CT). No significant changes were observed in the FTIR spectrum of the grafted ABS after further purification, indicating that the procedure was effective.

Determination of grafting degree of maleic anhydride

The grafting degree (GD) of MAH was determined by the back-titration procedure. A purified sample (1.0 g) was dissolved in 100 mL acetone, and then 10 mL ethanol solution of NaOH (0.1 mol/L) was added. The mixed solution was refluxed for 30 min under stirring, then back-titrated with HCl (0.1 mol/L) using methyl red as the indicator.

GD was defined as the amount of grafted maleic anhydride as a percentage of ABS-*g*-MAH and calculated by

$$\mathrm{GD}\ (\%) = \frac{(V_0 - V_1) \times 10^{-3} \times C \times M}{2W} \times 100$$

where V_0 is the amount of HCl consumed by using pure ABS as reference (mL), V_1 is the amount of HCl consumed by the grafted sample (mL), C is the molar concentration of HCl (mol/L), M is the molecular weight of maleic anhydride, and W is the weight of sample (g).

Melt flow index (MFI)

MFI values of ABS-*g*-MAH and raw ABS were determined according to the standard method at 200°C and 5 kg (5MPCA; Ray-Ran).

Differential scanning calorimeter

Calorimetric measurements were performed using a Perkin–Elmer PYRIS-1 differential scanning calorimeter (DSC). Transition temperatures were calibrated using indium and zinc standards. All scans were performed under an inert (N_2) atmosphere at a scanning rate of 10°C/min.

Impact test

All materials were compression molded in a 2-mm-thick plate at 210°C for 5 min. The size of the specimens was 100 × 40 × 2 mm. The notch was cut by a notch instrument (Ray-Ran). The Izod notch impact strength was measured by Izod instrument (Ray-Ran).

Tensile test

All materials were compression molded in a 2-mm-thick plate at 210°C for 5 min, and were grooved by a rotating to make dumbbell-type specimens whose dimensions of the parallel part were 20 mm in length with a cross section of 10 × 1 mm^2.

Tensile tests were conducted on a Universal Testing Machine (Instron 4465; Instron, Canton, MA) at a constant crosshead speed of 50 cm/min at 20°C and 80% RH.

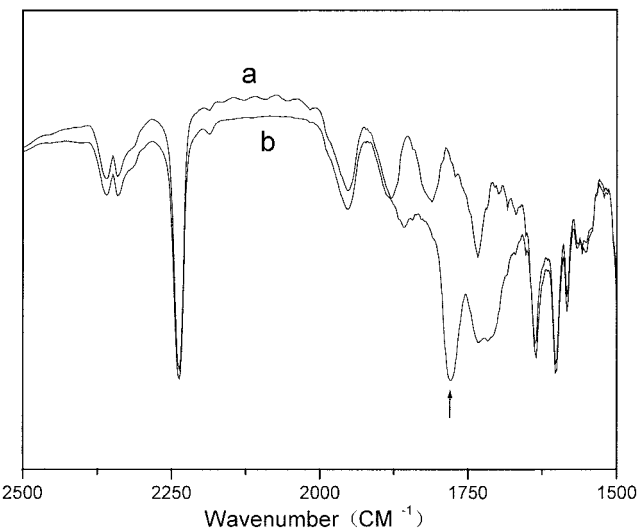

Figure 1 FTIR spectra of raw ABS and ABS-*g*-MAH: (a) raw ABS; (b) ABS-*g*-MAH (ABS = 100 g, DCP = 0.4 g, BPO = 0.2 g, MAH = 3 g; reactive temperatures: 185/190/190/190°C; screw speed: 30 rpm).

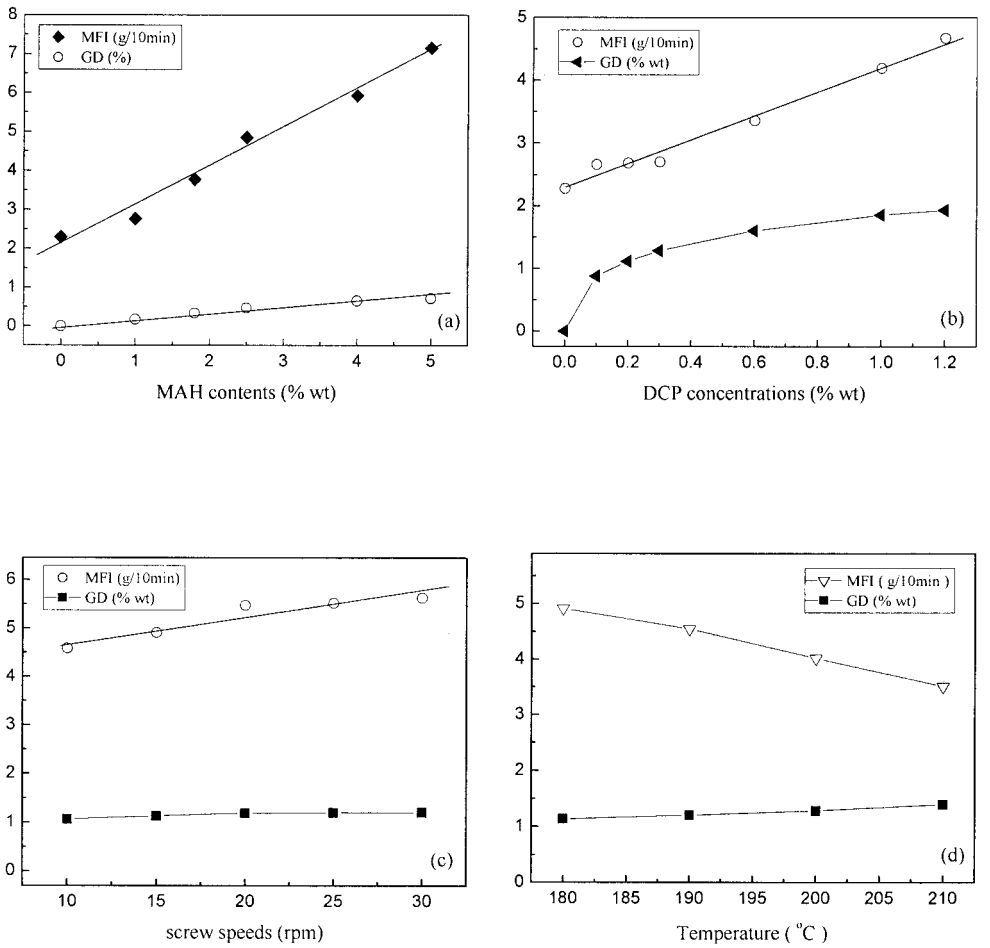

Figure 2 Effect of various factors on degree of grafting and melt flow index: (a) Effect of MAH content (ABS = 100 g, DCP = 0.3 g, BPO = 0.2 g; reactive temperatures: 190/190/190/190°C; screw speed: 20 rpm). (b) Effect of DCP concentration (ABS = 100 g, DCP : BPO = 3 : 2, MAH = 3 g; reactive temperatures: 185/190/190/190°C; screw speed: 20 rpm). (c) Effect of screw speed (ABS = 100 g, DCP = 0.3 g; BPO = 0.2 g, MAH = 3 g; reactive temperatures: 190/190/190/190°C). (d) Effect of reaction temperature (ABS = 100 g, DCP = 0.3 g, BPO = 0.2 g, MAH = 3 g; screw speed: 20 rpm).

Morphology

Scanning electron microscopy (SEM)

The morphology was examined by SEM. The SEM micrographs were obtained by a Hitachi S-2150 type SEM instrument (Hitachi, Ibaraki, Japan) at 25 kV. A vacuum unit was used to deposit a thin layer of metallic gold on the specimens.

Transmission electron microscopy (TEM)

The purified materials were dissolved in 1,2-dichloroethane, and then ultrathin films were prepared using distilled water. The rubber in the ABS phase was stained dark by an osmium tetraoxide (OsO_4) solution. The microstructure of the grafted and raw materials was analyzed by using a Philips CM-120 type TEM instrument (Philips, The Netherlands).

TABLE I
T_g of Raw ABS and ABS-*g*-MAH

	ABS747s	1	2	3	4
GD wt %		0.906	1.285	1.605	1.931
T_g (°C)	112.0	110.3	112.6	109.7	112.9

RESULTS AND DISCUSSION

Figure 1 shows the FTIR spectra of raw ABS and grafted ABS. Contrasted to the FTIR of raw ABS [Fig. 1(a)], the appearance of a new absorbance peak at 1780 cm^{-1} (C═O stretching from anhydride) in grafted ABS [Fig. 1(b)] indicates that the maleic anhydride was successfully introduced onto ABS.

Chemical modification usually influences the flow properties because of the side reactions such as crosslinking or degradation of polymer chains. Figure 2 displays the relationship of various reaction conditions and the GD of ABS-*g*-MAH, from which we can see that with the increase of the maleic anhydride

TABLE II
Mechanical Properties of Raw ABS and ABS-*g*-MAH

Properly	ABS747s	a	b	c	d	e	*F*
GD (wt %)	0	0.384	0.549	0.906	1.285	1.605	1.931
Tensile strength (MPa)	34.68	34.71	34.80	34.87	34.99	35.28	35.41
Elongation at break (%)	4.788	4.759	4.345	4.216	4.041	3.930	3.896

content, screw speed, temperature, and initiator content, the GD of ABS-*g*-MAH slightly increases because of using the binary initiator (see detailed discussion in our previous work[18]). Further studies indicated that the reactive condition such as the maleic anhydride content, screw speed, temperature, and initiator content also influenced MFI as well as GD. From Figure 2, we can see that the MFI increased with the increase of MAH content, DCP/BPO concentration, and screw speed, and fitted well to a linear relationship, whereas the MFI decreased almost linearly with the increase of temperature. We can also find that the MFI of ABS-*g*-MAH was higher than that of raw ABS in various reaction conditions because the grafted copolymerization may be accompanied by degradation of polymer chains. In the various reaction conditions, the effect of MAH content on MFI [shown in Fig. 2(a)] is the most noticeable because it has been well recognized that the degradation of ABS can enhance the MFI and some small amount of residual MAH also increases the MFI through a lubricant effect. As DCP and BPO (a fixed DCP/BPO weight ratio = 3 : 2) concentrations and screw speed increase, the MFI increases. In the reaction process, the degradation and the grafting of polymer both existed, and the MFI increases when the degradation of ABS is more prominent. The MFI decreased with increasing temperature because the grafted copolymerization surpassed the degradation at higher temperature.

Table I lists the T_g values of ABS-*g*-MAH and raw ABS, from which we can see that the T_g of ABS-*g*-MAH is almost identical to that of raw ABS. This is because the grafted copolymerization of MAH and the degradation of ABS both affect T_g.

The tensile strength and elongation ratio at fracture of ABS-*g*-MAH are shown in Table II. It has been shown that the tensile strength increased slightly with the increasing grafting degree and the percentage elongation at break decreased slightly with increasing GD. The impact strength of ABS-*g*-MAH decreased as

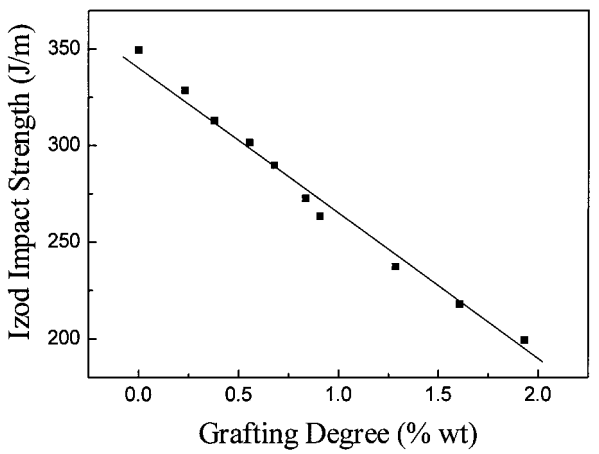

Figure 3 Effect of grafting degree on Izod impact strength for ABS-*g*-MAH.

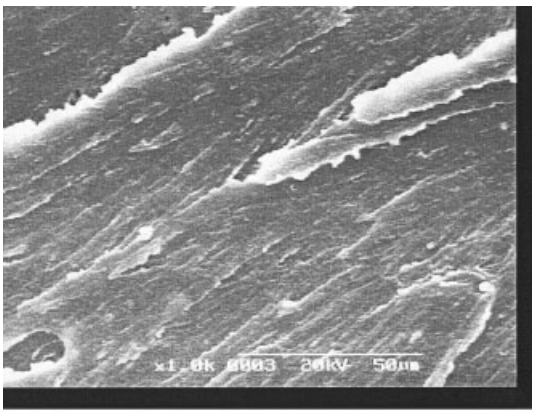

(a)

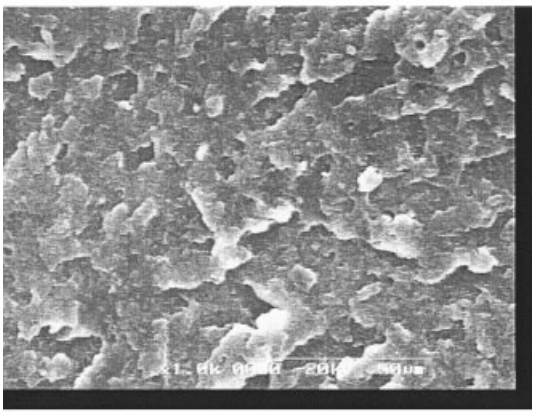

(b)

Figure 4 SEM micrographs of fracture surface of the samples: (a) raw ABS; (b) ABS-*g*-MAH (GD = 1.6 wt %).

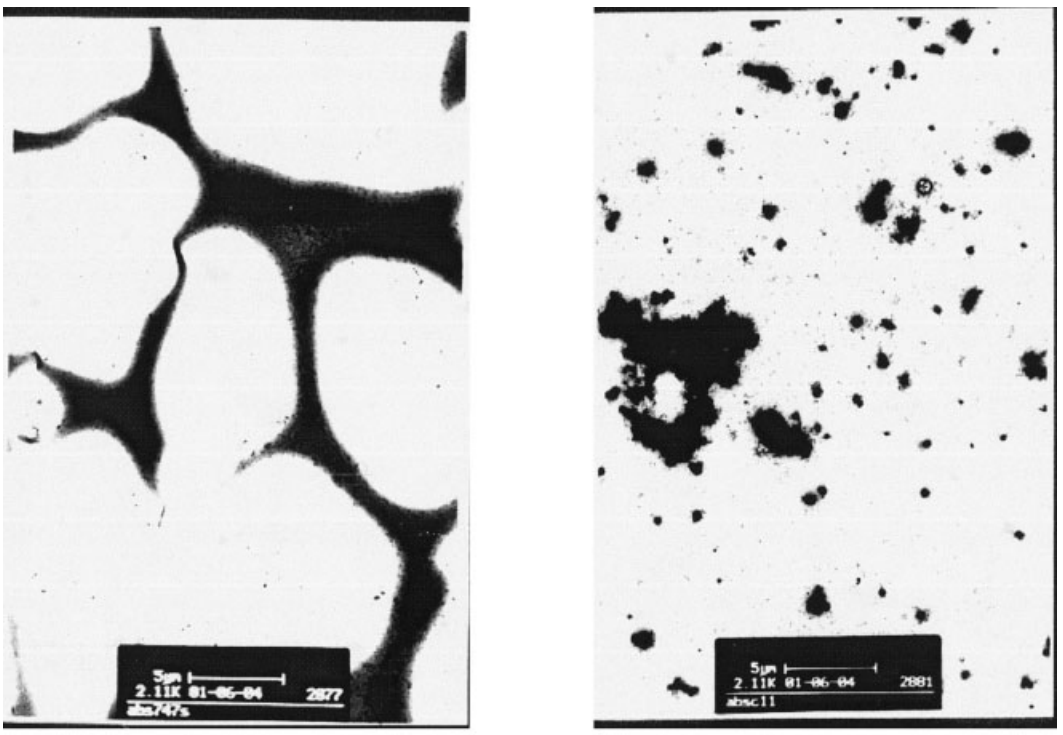

Figure 5 TEM photomicrographs of the samples: (a) raw ABS; (b) ABS-*g*-MAH (GD = 1.6 wt %).

the grafting degree increased, as shown in Figure 3, which may be explained by the grafting reaction occurring most likely in the butadiene region of ABS, which is also reported in Chandrasiri's work[8] and our previous work,[18]; thus the contents of the butadiene region (rubber region) are decreased with increased GD. In addition, the MAH molecule is rigid. Therefore, the toughness of ABS-*g*-MAH is reduced and the rigidity of ABS-*g*-MAH is increased slightly as the GD increased.

Fracture surfaces of the raw ABS and ABS-*g*-MAH are shown in Figure 4, from which we can see that the fracture type of ABS-*g*-MAH is the typical fractural break and that of the raw ABS is more ductile. This fact confirms that the ductility of ABS-*g*-MAH is reduced with increased grafting degree.

To further investigate the morphology of the raw ABS and ABS-*g*-MAH, the purified materials were dissolved in 1,2-dichloroethane, and then ultrathin films were prepared using distilled water. The films were stained with an OsO_4 solution in which rubber particles were uniformly stained. Figure 5(a) represents the morphology of raw ABS, which contains styrene–acrylonitrile (SAN) particles of a salami structure with rubber occlusions; meanwhile in the SAN region a few rubber particles of a salami structure exist. Figure 5(b) shows the morphology of ABS-*g*-MAH, which contains rubber particles of a salami structure with SAN occlusions, from which we can see that the phase structure in ABS-*g*-MAH is reversed. According to our previous work[18] and Chandrasiri's reports,[8] the grafting most probably occurs in the butadiene region of ABS, and so the content of the butadiene region (rubber region) is decreased with increased grafting degree, which may lead to the reverse of the phase structure. The rubber particles of a salami structure with SAN occlusions as grafting may also be consistent with the results that the ductility of ABS-*g*-MAH is decreased with increasing GD.

CONCLUSIONS

Infrared (IR) spectra confirmed that maleic anhydride was successfully grafted onto the ABS backbone in the molten state using dicumyl peroxide and benzoyl peroxide as the binary initiator and styrene as the comonomer. The changes of melt flow index, thermal properties, mechanical properties, and phase morphology in the graft copolymer were investigated. We found that reactive conditions such as the maleic anhydride content, screw speed, temperature, and initiator contents all influenced MFI as well as GD. The T_g of ABS-*g*-MAH was almost unchanged compared to that of raw ABS. The impact strength and the percentage elongation of ABS-*g*-MAH were decreased and the tensile strength of ABS-*g*-MAH was increased slightly

as the grafting degree increased. The phase structure of ABS-*g*-MAH was reversed compared with that of the raw ABS.

This work was financially supported by the Natural Science Foundation of China (No. 50390095). The authors are also grateful to Prof. Jie Yin, Prof. Chengxue Zhao, and Dr. Wei Yu for their beneficial suggestions on this manuscript.

References

1. Ide, F.; Hasegawa, A. J Appl Polym Sci 1974, 18, 963.
2. Huang, N. J.; Sundberg, D. C. J Polym Sci Part A: Polym Chem 1995, 33, 2533.
3. Brydon, A.; Burnett, G. M.; Cameron, G. G. J Polym Sci Polym Chem Ed 1974, 12, 1011.
4. Cameron, G. G.; Qureshi, M. Y. J Polym Sci Polym Chem Ed 1980, 18, 3149.
5. Manaresi, P.; Passalacqua, V.; Pilati, F. Polymer 1975, 16, 520.
6. Pham, B. T. T.; Tonge, M. P.; Monteiro, M. J. Macromolecules 2000, 33, 2383.
7. Chandrasiri, J. A.; Wilkie, C. A. J Polym Sci Part A: Polym Chem 1996, 34, 1113.
8. Rao, B. M.; Rao, P. R.; Sreenivasulu, B. Polym Plast Technol Eng 1999, 38, 967.
9. Zhou, Z. F.; Huang, H.; Liu, N. C. Eur Polym J 2001, 37, 1967.
10. Zhou, Z. F.; Huang, H.; Liu, N. C. J Polym Sci Part A: Polym Chem 2001, 39, 486.
11. Jiang, D. D.; Wilkie, C. A. Eur Polym J 1998, 34, 997.
12. Abdel-Razik, E. A. J Photochem Photobiol A Chem 1992, 69, 121.
13. Abdel-Razik, E. A.; Ali, M. M.; Abdelaal, M. Y.; Sarhan, A. A. Polym Plast Technol Eng 1996, 35, 865.
14. Scffaro, R.; Carianni, G.; La Mantia, F. P.; Zerroukhi, A.; Mignard, N.; Granger, R.; Arsac, A.; Guillet J. J Polym Sci Part A: Polym Chem 2000, 38, 1795.
15. Höelderle, M.; Bruch, M.; Luechow, H.; Gronski, W.; Müelhaupt, R. J Polym Sci Part A: Polym Chem 1998, 36, 1821.
16. Moad, G. Prog Polym Sci 1999, 24, 81.
17. Rodríguez-González, F. J.; Ramos-deValle, L. F.; Navarro-Rodríguez, D. ANTEC Tech Papers 1995, 43, 2076.
18. Qi, R. R.; Qian, J. L.; Zhou, Ch. X. J Appl Polym Sci 2003, 90, 1249.